DNA-RNA Complementation on Silicon Wafer for Thyroid Cancer Determination

Subash C.B. Gopinath[1,2] and Shijin Xuan[3*]

Running title: DNA-RNA Complementation on Silicon Wafer

[1]School of Bioprocess Engineering, 02600 Arau, [2]Institute of Nano Electronic Engineering, 01000 Kangar, Universiti Malaysia Perlis, Perlis, Malaysia.
[3]Department of Mammary and Thyroid Surgery, Jinan Central Hospital Affiliated to Shandong First Medical University, No.105, Jiefang road, Lixia District, Jinan, Shandong Province, 250013, P. R. China.

Subash C.B. Gopinath: subash@unimap.edu.my

Shijin Xuan: xyshijina@sina.com

***Correspondence:** xyshijina@sina.com

Abstract

One of the current issues with thyroid tumour is early diagnosis as it makes the higher possibility of curing. This research was focused to detect and quantify the level of specific target sequence complementation of miR-222 with capture DNA sequence on Interdigitated Electrode (IDE) sensor. The aluminum electrode with the gap and finger sizes of 10 µm was fabricated on silicon wafer, further the surface was amine-functionalized for accommodating carboxylated-DNA probe. With DNA-target RNA complementation, the detection limit was attained to be 1 fM as estimated by a linear regression analysis [$y = 1.5325x - 2.1171$ $R^2 = 0.9065$] and the sensitivity was at the similar level. Current responses were higher by increasing the target RNA sequence concentrations. Control experiments with mismatched/noncomplementary sequences were failed to complement the capture DNA sequence immobilized on IDE, indicating the specific target validation. This research helps diagnosing and identifying the progression with thyroid tumor and miRNA being a potential “marker” in atypia diagnosis.

Keywords: Thyroid tumor; microRNA; Biosensor: Interdigitated electrode; Duplex formation

Highlights

Focused to detect the specific target sequence complementation of miR-222 on Interdigitated Electrode (IDE) sensor at the level of 1 fM. Control experiments with mismatched/noncomplementary sequences were failed to complement the capture DNA sequence immobilized on IDE, indicating the specific target validation. This research helps diagnosing and identifying the progression with thyroid tumor and miRNA being a potential “marker” in atypia diagnosis.

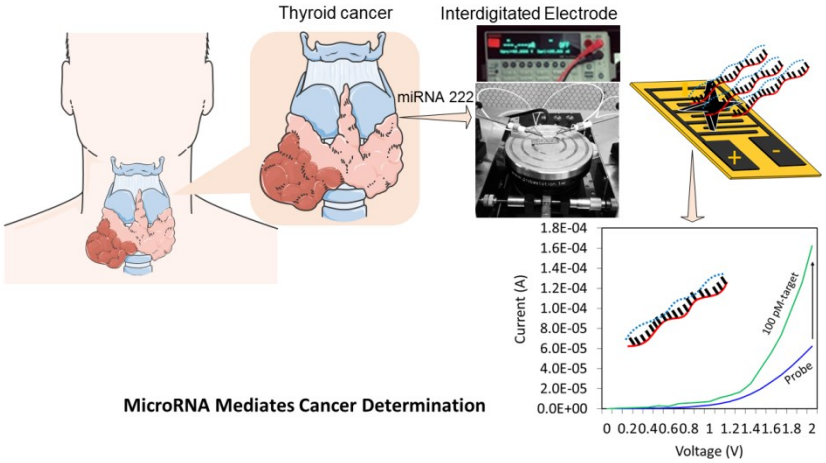

1. Introduction

Thyroid tumor is a malignant starts in the thyroid glands located in the front part of the neck and at the base of throat [1]. It starts with the healthy cells in the thyroid glands and grow without control to form the tumor [2]. In general, thyroid cancer has been diagnosed by the physical examination of the neck, X-rays and imaging systems and used to identify the thyroid tumor. Further, the suspicious patients undergo ultrasound guided fine needle aspiration [3]. The results of this procedure may show suspicious malignancy, follicular neoplasm or features of atypia in the diagnosis of thyroid nodules. Apart from that, these diagnostic methods are highly depending on the technician and operators.

Currently a decent number of biosensors for diagnosing thyroid are available predominantly with biochemical sensors [4,5]. Further developments have been shown recently with involving artificial intelligence and nanomaterial. These progresses made the way to produce high-performance sensors for diagnosing issues associated with thyroid [6–9]. Various blood-based biomarkers are supporting the diagnosis of thyroid tumor along with imaging system. Among them microRNAs (miRNAs) are found to be dysregulated in various types of cancers, including thyroid tumor [10–12]. miRNA based sensors have been

designed similar to the strategies followed in DNA-based sensors. Both are working with the formation of complementation, however, the sequence from miRNA considered to be unique in the cellular system compared to the DNA and less populated, which makes miRNA as an attractive tool in recent days. miRNA is an endogenous, small, noncoding RNA, act as the negative regulators in gene expression [13,14]. It plays a major role in cell differentiation, cell growth, adhesion and apoptosis [15]. miRNA-222 is highly correlated with various types of cancers such as gastric cancer, bladder cancer, breast cancer, papillary thyroid cancer [16–19]. In particular, miRNA-222 has been found to be upregulated in the patient with thyroid tumor, additionally, it differentiate between malignant and benign nodules [20,21]. Detecting and quantifying the level of miRNA-222 helps to diagnose the thyroid tumor and follow-up treatments. The current research is focused to quantify the specific target sequence from miRNA-222 by complementing with capture probe. Capture DNA sequence was immobilized on interdigitated electrode (IDE) sensor through the amine-carboxylic acid linker and identified by target sequence.

IDE is an established transducing system, widely used in various applications, especially in the field of biosensor to diagnose the range of diseases by its easier fabrication process, inexpensive and higher-sensitivity [22,23]. These bring-out the inherent advantages with additional advantageous such as, portability, real-time output and the higher-performance [24–27]. In general, IDE sensor has been involved a selective recognition of biological elements; it converted into an electric-signal with the help of transducer. Targets for disease biomarkers, such as DNA, RNA, protein, peptide, and receptor were successfully identified by using IDE sensor by its lower detection level using appropriate probes (aptamer/antibody) [28–31]. In

this research COOH-terminated capture DNA sequence was immobilized on amine-modified IDE and detected by complementing the target miRNA-222.

2. Materials and methods

2.1. Reagents and biomolecules

Phosphate buffered saline (PBS) and (3-Aminopropyl)triethoxysilane (APTES) were purchased from Sigma-Aldrich (USA). Ethanolamine was purchased from Fisher Scientific (UK)**.** All oligos were commercially synthesized and supplied from Apical Scientific Sdn. Bhd. (Malaysia). The designed oligos are from Bettazzi et al. (2013) [20] as follows: Target (miRNA-222) RNA sequence: 5′-AGCUACAUCUGGCUACUGGGUCUC-3′ (18 mer); Probe sequence: 5′-COOH-C6-GAGACCCAGTAGCCAGATGTAGCT-3′ (18 mer); Noncomplementary: 5′-UCGAUGUAGACCGAUGACCCAGAG-3′ (18 mer); Three-mismatch sequence (underlined): 5′-AGCUACAUCUCCGUACUGGGUCUC-3′ (18 mer).

2.2. IDE sensor surface fabrication

IDE sensor was fabricated on silicon wafer by applying the traditional wet-etching method as in the previous study [32]. The procedure for fabrication was involved 7 mandatory steps: (i) silicon wafer was oxidized to form silicon di-oxide layer by the thermal oxidation [at 500° C; 1 h]; (ii) On this oxidized surface aluminum was layered by using the thermal evaporator; (iii) Spin-coater was used to coat with positive photo-resist; (iv) UV-exposure was utilized to transform the pattern by the photoresist; (v) Unexposed area was removed by using the resist developer; (vi) Unexposed aluminum layer was eliminated by immersing the electrode in an aluminum etchant solution; (vii) Finally, fabricated IDE was washed with acetone followed by distilled water.

2.3. Carboxylated-capture DNA immobilization

COOH-linked capture DNA was immobilized on IDE sensor through the amine (silane) modification. Initially, the surface of IDE was hydrolyzed for 1 min with 1% of KOH. Two percent of APTES was diluted in 30% ethanol and dropped on the hydrolyzed IDE sensor and rested it for 2 hr. Washed the surface with 30% ethanol and double distilled water thoroughly to remove the excess APTES. Then, 1 μM of diluted COOH-capture DNA in PBS was placed on amine-modified IDE sensor and kept for 1 h at RT (activation step was preferred). The surface was washed five times with PBS buffer and then the excess amine surface was blocked by 1 M ethanolamine to avoid the nonspecific binding. These COOH-capture DNA immobilized surfaces were utilized to detect the target DNA complementation of the designed sequence from miRNA-222.

2.4. Determination of target RNA complementation

Hundred picomolar of the diluted target RNA sequence (miRNA-222) was dropped on COOH-capture DNA modified IDE sensor and kept for 30 min to form a duplex formation. After the surface washed with PBS buffer, the changes in current were noted. The current difference between before and after the duplex was considered as the real interaction of capture-DNA and target-RNA. To find the limit of detection, target RNA concentrations with 100 aM, 1 fM, 10 fM, 100 fM, 1 pM, and 10 pM were duplexed individually on COOH-capture DNA modified IDE sensor and then the current reading was noted after 30 min incubation followed by the washing step. The difference in current for each target RNA concentration was plotted in an excel sheet as a linear regression graph to estimate the limit of detection. Limit of detection was considered from the calibration line at low concentrations against the background

signal (Signal-to-noise as 3:1) and estimated (standard deviation of the baseline + 3σ).

2.5. Control experiments for the specific detection of target RNA complementation

Control experiments were performed with triple mismatch and noncomplementary RNA sequences of target for miRNA-222. In addition, the surface with no capture-DNA sequence against the specific target was tested. A 1 μM of these sequences was complexed on COOH-capture DNA modified IDE sensor. The changes in current before and after immobilizations were noted. This current change was compared with the specific complementation of capture DNA and target RNA.

3. Results and Discussion

There are different ways have been followed for the interaction of biomolecules towards the validation of disease biomarkers on the sensing surfaces [33–35]. These interactions include, protein-protein, protein-antibody, protein-aptamer, DNA-DNA, DNA-RNA, probe-receptor, probe-glycan, probe-lipid. With these wide range options, panels of biosensors were generated [11,36–39]. However, the preferences fall with the affinity between the desired target molecule/biomarker of interest against the probe, which can capture the targeted molecule. In the current investigation, RNA sequence was targeted to complex with DNA as the capturing probe for determining thyroid tumour on the interdigitated electrode (IDE) sensor (Figure 1).

The target RNA sequence from miRNA-222 was identified on IDE sensor surface towards diagnosing thyroid cancer. The dimensions of IDE surface are with, a length of 7500 μm; a width of 4100 μm; 20 finger-gap pairs; a gap size of 85 μm; electrode size of 100 μm; electrode thickness of 40 nm; and a finger length of 4000 μm. Figure 2 shows the graphical illustration of surface immobilization of the capture

DNA and its duplex with the target RNA (miRNA-222) on IDE sensor. Initially, the fabricated aluminium electrode on the silicon wafer was validated under high-power microscopy and measured the finger and gap regions to be 10 μm. IDE surface was modified into amine by using 2 % of APTES and then COOH-terminated capture DNA was attached. COOH in capture DNA interacts with amine on IDE through the chemical-coupling. Capture DNA molecule immobilization is playing a crucial role in improving the limit of detection. Higher and proper immobilization of capture molecule attracts higher number of target sequences. Our earlier research biotin and tetravalent streptavidin complex strategy was used to immobilize the capture DNA on IDE sensor, but it involves more steps and leads to an increased experimental timing. In the current work, capture DNA was directly immobilized on IDE sensor through one step chemical-coupling of capture DNA and surface of IDE. This method minimizes the experimental step and cost. On the DNA captured sensor surface, target RNA sequence from miR-222 was detected and calculated the detection limit.

3.1. Confirmation of COOH-capture DNA immobilization

COOH-capture DNA [5′-COOH-C6-GAGACCCAGTAGCCAGATGTAGCT-3′] immobilization was confirmed by measuring the changes in the current level on IDE sensor (Figure 3a). APTES modified IDE was showing the current level to be 1.57E-07 A, after drop the COOH-capture DNA, the current was increased to 5.37E-07 A. The difference in current was noted as 3.8E-07 A. This increment in current was clearly declared the chemical-coupling of amine on IDE with COOH-terminated capture DNA.

3.2. Detection of miRNA-222 on capture DNA-modified IDE

The surface of IDE was blocked with ethanolamine before detecting the target DNA sequence [5′-AGCUACAUCUGGCUACUGGGUCUC-3′] in order to avoid the nonspecific binding. After adding the ethanolamine, the current was increased a little higher to 6.23E-05 A. This minimal increment was due to the ethanolamine attachment on the remaining IDE sensor surface, which is free from the capture DNA. This capture DNA modified IDE was utilized to detect miR-222 target RNA sequence on IDE sensor. As shown in figure 3b, after adding 100 pM of target RNA, the level of current was increased to 1.63 E-04 A. The difference in current was noted as 10.2 E-07 A. This current increment was confirmed the duplex formation from capture DNA and target RNA sequences.

3.3. Limit of detection with target miRNA-222 complementation

To calculate the limit of detection with target (miRNA-222) complementation, different concentrations of target RNA and capture DNA duplex formation was calculated on IDE sensor. For that 100 aM to 10 pM of target RNA concentrations were titrated and interacted individually on COOH-capture DNA immobilized IDE sensor. As shown in figure 4a, after drop 100 aM of target, the current response was increased from 6.23E-05 to 6.84E-05 A. The difference in current change was noted as 0.61E-05 A. This increment in current was confirmed the detection of 100 aM of target RNA on capture DNA modified IDE sensor. Further, 1 fM, 10 fM, 100 fM, 1 pM, 10 pM were tested and the current responses were to 7.45 E-05, 7.96E-05, 9.02E-05, 1.10E-04 and 1.30E-04 A, respectively. As revealed from the current responses, with increment in the target concentrations, the responses in currents were gradually increased (Figure 4b). These changes caused the difference in

current were noted as 1.22, 1.73, 2.79, 4.77, and 6.77 E-07 A, respectively. This difference was plotted in a linear regression graph, and calculated the limit of detection of target was 1 fM. Further, the sensitivity was also falling under the similar level (Figure 5a).

3.4. Control experiments for the specific detection of target miRNA-222

Control experiments were carried out to confirm our system that can specifically detect the target RNA sequence. Two sequences namely, triple mismatch [5′-AGCUACAUCUCCGUACUGGGUCUC-3′] and noncomplementary [5′-UCGAUGUAGACCGAUGACCCAGAG-3′] of the desired RNA target sequences were dropped individually on COOH-capture DNA immobilized IDE sensor and the changes in current were noted. Similarly, the specific sequence [5′-AGCUACAUCUGGCUACUGGGUCUC-3′] was tested on the IDE surface without capture DNA probe. As shown in figure 5b, all control experiments were failed to show any significant current responses confirming the specific detection of target and no nonspecific binding.

4. Conclusion

This research was focused to determine the thyroid tumor by detecting the blood-based biomarker, miRNA-222 on interdigitated electrode (IDE) sensor. COOH-capture DNA was chemically immobilized on IDE sensor surface. Target sequence from miR-222 was duplexed on capture DNA sequence modified surface, and confirmed by measuring the changes in the current response. The limit of detection and sensitivity with target RNA and capture DNA interaction were calculated as 1 fM, and with increasing target concentrations, the responses in current were increased. In addition, control sequences [noncomplementary and triple mismatch sequences]

of target did not show the significant changes in current response, which confirmed the specific detection. This experimental detection of miRNA-222 helps to determine thyroid tumor and its progression.

Competing interests

The authors declare that they have no competing interests.

Author Contributions

Subash C.B. Gopinath: Conceptualization; Methodology; Validation; Investigation; Visualization; Data Curation; Writing—original draft; Writing-Reviewing and Editing.

Shijin Xuan: Formal analysis; Validation; Investigation; Visualization; Data Curation; Supervision; Funding; Writing-Reviewing and Editing

Acknowledgements

Thanks to Smart Servier Medical Art for reproducing their available images.

References

[1] Davies, L., and Welch, H.G. (2006) J. Am. Med. Assoc., 295, 2164-2167.

[2] Grimm, D. (2017) Int. J. Mol. Sci., 18, 1529.

[3] Gupta, M., Gupta, S., and Gupta, V.B. (2010) J. Thyroid Res., 2010, 379051.

[4] Wang, H., Wu, X., Dong, P., Wang, C., et al. (2014) Int. J. Electrochem. Sci., 9, 12–21.

[5] Pacheco, J.G., Rebelo, P., Cagide, F., Gonçalves, L.M., et al. (2019) Talanta, 194, 689–696.

[6] Rajesh, Kumar, K., Mishra, S.K., Dwivedi, P., and Sumana, G. (2019) TrAC - Trends Anal. Chem. 2019, 666–676.

[7] Sharma, S., Aguilera, R., Rao, J.Y., and Gimzewski, J.K. (2019) Sci. Rep. 9, 9282.

[8] Nguyen, D.T., Kang, J.K., Pham, T.D., Batchuluun, G., and Park, K.R. (2020) Sensors (Switzerland) 20, 1822.

[9] Omer, W.E., El-Kemary, M.A., Elsaady, M.M., Abou-Omar, M.N., et al., (2020) ACS Omega 5, 5629–5637.

[10] Yu, S., Liu, Y., Wang, J., Guo, Z., et al., (2012) J. Clin. Endocrinol. Metab. 97, 2084–2092.

[11] Cardoso, A.R., Moreira, F.T.C., Fernandes, R., and Sales, M.G.F. (2016) Novel and simple electrochemical biosensor monitoring attomolar levels of

miRNA-155 in breast cancer. Biosens. Bioelectron. 15, 621–630.

[12] Aghili, Z., Nasirizadeh, N., Divsalar, A., Shoeibi, S., and Yaghmaei, P. (2017) A highly sensitive miR-195 nanobiosensor for early detection of Parkinson's disease. Artif. Cells, Nanomedicine Biotechnol. 2017, 1–9.

[13] Cheng, Y., Dong, L., Zhang, J., Zhao, Y., and Li, Z. (2018) Analyst 2018, 1758–1774.

[14] Park, N.J., Zhou, H., Elashoff, D., Henson, B.S., et al., (2009) Clin. Cancer Res. 15, 5473–5477.

[15] Wahid, F., Shehzad, A., Khan, T., and Kim, Y.Y. (2010) Biochim. Biophys. Acta - Mol. Cell Res. 2010, 1231–1243.

[16] Kim, Y.K., Yu, J., Han, T.S., Park, S.Y., et al. (2009) Nucleic Acids Res. 37, 1772–1681.

[17] Puerta-Gil, P., Garca-Baquero, R., Jia, A.Y., Ocaa, S., et al., (2012) Am. J. Pathol. 180, 1808–1815.

[18] Di Leva, G., Gasparini, P., Piovan, C., Ngankeu, A., et al., (2010) J. Natl. Cancer Inst. 102, 706–721.

[19] Lee, J.C., Zhao, J.T., Gundara, J., Serpell, J., et al. (2015) J. Surg. Res. 196, 39–48.

[20] Bettazzi, F., Hamid-Asl, E., Esposito, C.L., Quintavalle, C., et al. (2013) Anal. Bioanal. Chem. 405, 1025–1034.

[21] Pallante, P., Visone, R., Ferracin, M., Ferraro, A., et al., (2006) Endocr. Relat. Cancer 13, 497–508.

[22] Ohno, R., Ohnuki, H., Wang, H., Yokoyama, T., et al. (2013) Biosens. Bioelectron. 40, 422–426.

[23] Guo, S., Li, Y., Li, R., Zhang, P., et al., (2019) Biotechnol. Appl. Biochem. 2019, 1–7.

[24] Zhang, R., Wang, S., Huang, X., Yang, Y., et al., (2020) Anal. Chim. Acta 1094, 142-150.

[25] Letchumanan, I., Gopinath, S.C.B., and Arshad, M.K.M., (2020) Microchim. Acta 187, 128.

[26] Wang, Y., Guo, Y., Lu, J., Sun, Y., et al. (2020) Nanoscale Res. Lett. 15, 33.

[27] Zhang, J., and Gopinath, S.C.B. (2020) 3 Biotech 10, 35.

[28] Zheng, S., Zhang, H., Lakshmipriya, T., Gopinath, S.C.B., and Yang, N. (2019) Biomed Res. Int. 2019, 9726967.

[29] Lv, Q., Wang, Y., Su, C., Lakshmipriya, T., et al. (2019) Int. J. Biol. Macromol. 134, 354–360.

[30] Lin, J., Gopinath, S.C.B., Lakshmipriya, T., Chen, Y., et al. (2019) Int. J. Biol. Macromol. 141, 564–569.

[31] Letchumanan, I., Md Arshad, M.K., Balakrishnan, S.R., and Gopinath, S.C.B. (2019) Biosens. Bioelectron. 130, 40–47.

[32] Ramanathan, S., Gopinath, S.C.B., Md Arshad, M.K., Poopalan, P., et al. (2019) Appl. Phys. A 125, 548.

[33] Diculescu, V.C., Paquim, A.M.C., and Brett, A.M.O. (2005) Sensors 2005, 377–393.

[34] Jang, H.J., Lee, T., Song, J., Russell, L., et al., (2018) ACS Appl. Mater. Interfaces 10, 16233–16237.

[35] Yang, C., Denno, M.E., Pyakurel, P., and Venton, B.J. (2015) Anal. Chim. Acta 2015, 17–37.

[36] Luan, Y., Lu, A., Chen, J., Fu, H., and Xu, L. (2016) Appl. Sci. 6, 432.

[37] Liu, F., Zhang, J., Chen, R., Chen, L., and Deng, L. (2011) Chem. Biodivers. 8, 311–316.

[38] Zuo, X., Song, S., Zhang, J., Pan, D., et al., (2007) J. Am. Chem. Soc. 129, 1042–1043.

[39] Ng, A.H.C., Uddayasankar, U., and Wheeler, A.R., (2010) Anal. Bioanal. Chem. 397, 991–1007.

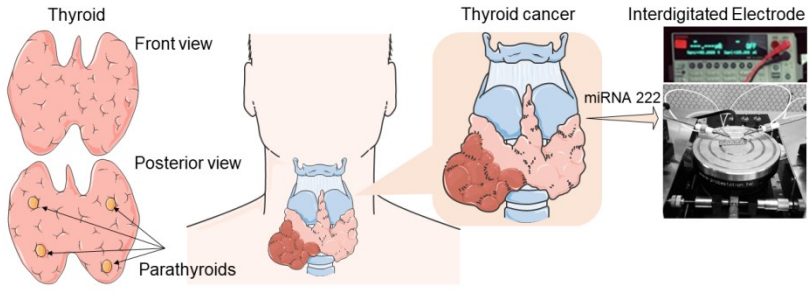

Figure 1: Overview on thyroid cancer and detection. miRNA-222 based detection on IDE is shown.

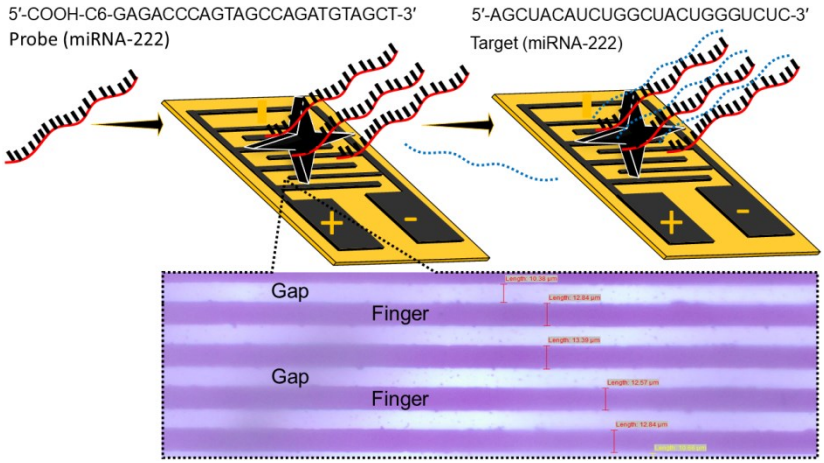

Figure 2: Diagrammatic representation for the detection of miRNA-222. DNA-RNA based detection is shown. IDE sensing surface observed under high-power microscopy is displayed.

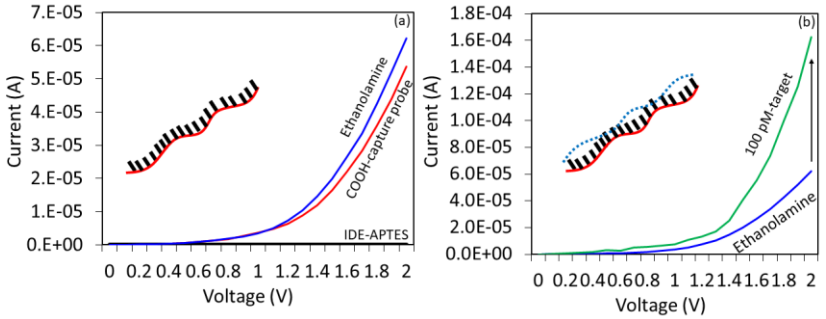

Figure 3: Preliminary assessment on measurements. (a) Surface chemical functionalization. (b) Probetarget interaction. 100 pM of the target was tested. Arrow indicates the direction of current changes. Figure inserts are diagrammatic representation.

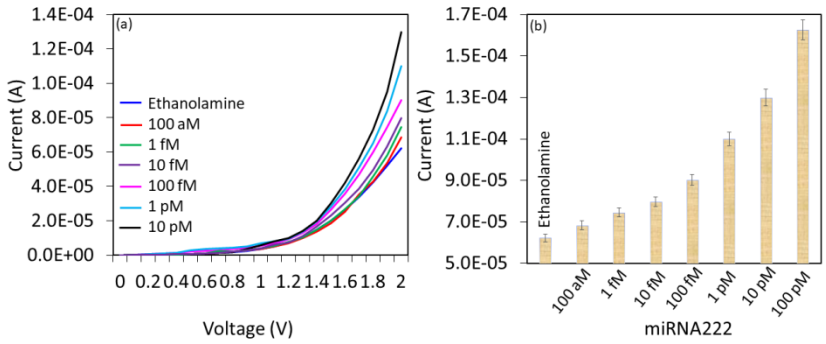

Figure 4

Figure 4: Dose-dependent analysis. (a) Concentration-dependent current changes. Concentrations from 100 aM until 10 pM were tested. (b) Averaged data. Values were averaged by triplicates (n=3).

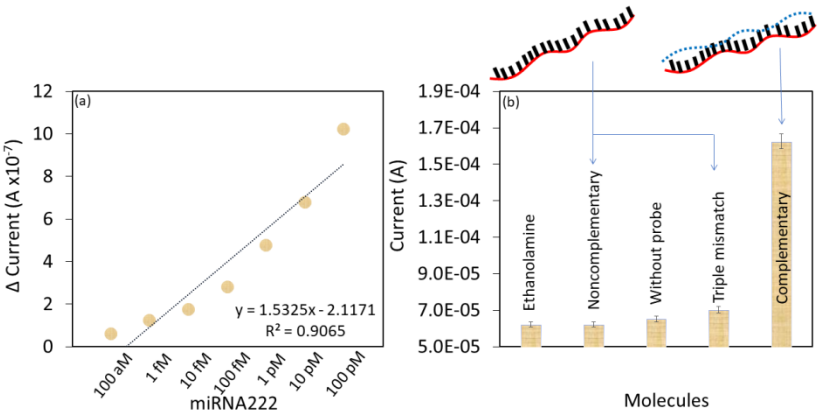

Figure 5

Figure 5: High-performance analysis. (a) Linear regression analysis. R-squared value was estimated to be 0.9065. (b) Specificity analysis. Noncomplementary, triple-mismatched sequences and detection in the absence of probe were compared with the specific detection. Figure inserts are diagrammatic representation.